Electronic Supplementary Material (ESI) for Dalton Transactions.

Supporting Information

Uranyl phosphonates: crystalline materials and nanosheets for temperature sensing

Ge-Hua Wen,[a] Xiu-Mei Chen,[b] Kui Xu,[a] Xiaoji Xie,[b] Song-Song Bao,[a*] and Li-Min Zheng*[a]

Table S1. Selected bond lengths (Å) and angles (°) for **1**.

Bond	Length [Å]	Bond	Length [Å]
U1–O6	1.763(3)	O6A–U1–O1A	90.41(13)
U1–O6A	1.763(3)	O6–U1–O2B	88.91(13)
U1–O1	2.299(3)	O6A–U1–O2B	91.09(13)
U1–O1A	2.299(3)	O1–U1–O2B	89.35(11)
U1–O2B	2.338(3)	O1A–U1–O2B	90.65(11)
U1–O2C	2.338(3)	O6–U1–O2C	91.09(13)
O6–U1–O1	90.41(13)	O6A–U1–O2C	88.91(13)
O6A–U1–O1	89.59(13)	O1–U1–O2C	90.65(11)
O6–U1–O1A	89.59(13)	O1A–U1–O2C	89.35(11)

Symmetric codes for **1**: A: -x+2, -y+1, -z; B: x+1, y, z; C: -x+1, -y+1, -z.

Table S2. The parameters of H-bonding for **1**.

D-H···A	$d_{H\cdots A}$(Å)	$d_{D\cdots A}$(Å)	$Angle_{D\text{-}H\cdots A}$(°)
O5-H5···O2[a]	2.08	2.919(5)	176.5
O13-H13···O4[a]	1.88	2.588(5)	140.4
C4-H4···O6[b]	2.68	3.381(6)	131.5
C5-H5A···O5[c]	2.91	3.843(6)	167.4

Symmetric codes for **1**: a: -x+1, -y+1, -z+1; b: x, -1+y, z; c: 2-x, -y, 1-z.

Table S3. Selected bond lengths (Å) and angles (°) for **2**.

Bond	Length [Å]	Bond	Length [Å]
U1-O1	2.511(6)	O6–U1–O3	156.6(2)
U1–O3	2.511(6)	O1A–U1–O3	66.0(2)
U1–O4	1.771(7)	O3A–U1–O3	121.81(17)
U1–O5	1.770(7)	O1–U1–O3	56.8(2)
U1–O6	2.221(7)	O10–U2–O9	178.6(3)
U1–O1A	2.364(7)	O10–U2–O8	91.9(3)
U1–O3B	2.374(7)	O9–U1–O8	89.1(3)
U2–O8	2.313(7)	O10–U2–O7C	91.0(3)
U2–O9	1.788(7)	O9–U2–O7C	88.5(3)
U2–O10	1.757(7)	O8–U2–O7C	157.4(2)
U2–O7C	2.322(7)	O9–U2–O2B	92.7(3)
U2–O2B	2.325(6)	O8–U2–O2B	79.1(2)
U2–O11D	2.455(7)	O7c–U2–O2B	78.6(2)
U2–O12D	2.511(7)	O10–U2–O11B	88.0(3)
O5–U1–O4	177.6(3)	O9–U2–O11D	91.3(3)
O5–U1–O6	93.1(3)	O8–U2–O11D	74.5(2)
O4–U1–O6	89.1(3)	O7c–U2–O11D	128.0(2)
O5–U1–O1A	89.0(3)	O2b–U2–O11D	153.2(3)
O4–U1–O1A	90.1(3)	O10–U2–O12D	89.3(3)
O6–U1–O1A	90.8(2)	O9–U2–O12D	89.3(3)
O5–U1–O3A	85.4(3)	O8–U2–O12D	126.6(2)
O4–U1–O3B	95.8(3)	O7c–U2–O12D	75.8(2)
O6–U1–O3B	81.6(2)	O2b–U2–O12D	154.3(2)
O1a–U1–O3B	170.2(2)	O11d–U2–O12D	52.2(2)
O5–U1–O1	93.2(3)	O10–U2–O16D	84.2(3)
O4–U1–O1	85.4(3)	O9–U2–O16D	94.6(3)
O6–U1–O1	146.1(2)	O8–U2–O16D	100.6(3)
O1a–U1–O1	122.63(18)	O7c–U2–O16D	102.0(3)
O3b–U1–O1	65.8(2)	O2b–U2–O16D	172.7(3)
O5–U–O3	88.7(3)	O11d–U2–O16D	26.2(3)
O4–U1–O3	88.9(3)	O12d–U2–O16D	26.6(3)

Symmetric codes for **2**: A: -x+1, y+1/2, -z+1/2; B: -x+1, y-1/2, -z+1/2; C: x, y-1, z; D: -x+1, -y+1, -z+1.

Table S4. The parameters of H-bonding for **2**.

D-H···A	$d_{H\cdots A}$(Å)	$d_{D\cdots A}$(Å)	$Angle_{D\text{-}H\cdots A}$(°)
O1W-H1WA···O9	2.01	2.884(12)	151.6
O1W-H1WB···O11	2.01	2.896(12)	154.8
O1W-H1WC···O7[a]	2.05	2.979(11)	166.7
O14-H14···O13[b]	1.77	2.603(12)	170.5

Symmetric codes for **2**: a: -x+1, -y+1, -z+1; b: -x+2, -y+1, -z+1.

Table S5. Inductively Coupled Plasm (ICP) analysis of **1** and **2** in the different aqueous solution.

Sample	**1**		**2**	
	P content (mg/L)	Dissociation degree (%)	P content (mg/L)	Dissociation degree (%)
pH=1	0.289	1	0.538	2.6
pH=4	0.320	1.1	0.017	0.08
pH=8	0.318	1.1	0.019	0.09
pH=10	0.434	1.5	0.141	0.7
HNO_3	7.68	8.8	3.05	5.0
H_2SO_4	0.73	3	0.76	1.2
aqua regia	22.4	25.8	9.1	14.7

1 mg of sample **1** or **2** was soaked in aqueous solution (3 mL) at variable pH (pH = 1, 4, 8, 10) for 24 h. After centrifuge (rpm 14000) and filter (Syringe filters, aperture: 0.22μm) of the mixture, the concentrations of P element in the filtrate were detected by ICP technique. 1 mg of sample **1** or **2** was soaked in fuming acids (1 mL), then tested by ICP after dilution ten times, the above values has been multiplied by ten.

Table S6. The lifetime fit parameters of **1, 2**, **1-ns@PMMA** and **2-ns@PMMA**.

1	τ_1(μs)	τ_2(μs)	$\tau_{average}$ (μs)	χ^2
77K	388.1, 30.3%	1110.1, 69.7%	891.2	1.10
300K	266.5, 28.7%	748.6, 71.3%	610.3	1.17

1-ns@PMMA	τ_1(μs)	τ_2(μs)	$\tau_{average}$ (μs)	χ^2
77K	310.4, 32.5%	1078.3,67.5%	828.5	1.10
300K	234.0, 29.5%	827.8, 70.5%	652.5	1.02

2	τ_1(μs)	τ_2(μs)	$\tau_{average}$ (μs)	χ^2
77K	35.6, 51.7%	113.6, 48.3%	73.2	1.11

2-ns@PMMA	τ_1(μs)	τ_2(μs)	$\tau_{average}$ (μs)	χ^2
77K	20.3, 59.4%	81.5, 40.6%	45.1	1.19

The fluorescence decay curve fitted by double-exponential function (eqn (1)) at different temperatures, respectively. The average lifetime is calculated using eqn (2).

$$\boldsymbol{I_{(t)} = A + B_1 \exp(-t/\tau_1)^{-1} + B_2 \exp(-t/\tau_2)^{-1}} \quad \textbf{(1)}$$

$$\boldsymbol{(t) = \left(B_1 {\tau_1}^2 + B_2 {\tau_2}^2\right)/(B_1\tau_1 + B_2\tau_2)} \quad \textbf{(2)}$$

Table S7. Comparison of the thermometer performance of **1**, **2** and **2-ns@PMMA** with some reported CP materials.

Materials	Temp. range [K]	Max. Sm % K^{-1}	References
TbMOF@7.3%Eu_tfac	200–325	1.33	1
ZJU-88⊃perylene	293-353	1.28	2
$Eu_{0.0069}Tb_{0.9931}$DMBDC	50-200	1.15	3
{[Tb(cpbOH)$(H_2O)_2$](cpb)}$_\infty$	180-280	1.84	4
{[Eu(cpbOH)$(H_2O)_2$](cpb)}$_\infty$	180-280	1.40	
$Tb_{0.9}Eu_{0.1}$PIA	100-300	3.27	5
$Tb_{0.99}Eu_{0.01}(BDC)_{1.5}(H_2O)_2$	290-320	0.31	6
$Tb_{0.8}Eu_{0.2}$BPD	298-318	1.19	7
$[Eu_{0.7}Tb_{0.3}(cam)(Himdc)_2(H_2O)_2]_3$	100-450	0.11	8
TbDyCo-MOF	120–200	2.2(3)	9
Na@U_6P_6	200-300	0.79	10
1	120-300	0.9	*This work*
2	100-300	2.16	*This work*
2-ns@PMMA	100-300	1.19	*This work*

References

1. A. M. Kaczmarek, Y.-Y. Liu, C. Wang, B. Laforce, L. Vincze, P. V. D. Voort and R. V. Deun, *Dalton Trans.*, 2017,**46**, 12717-12723.
2. Y. Cui, R. Song, J. Yu, M. Liu, Z. Wang, C. Wu, Y. Yang, Z. Wang, B. Chen and G. Qian, *Adv. Mater.*, 2015, **27**, 1420-1425.
3. Y. J. Cui, H. Xu, Y. F. Yue, Z. Y. Guo, J. C. Yu, Z. X. Chen, J. K. Gao, Y. Yang, G. D. Qian and B. L. Chen, *J. Am. Chem. Soc.*, 2012, **134**, 3979.
4. X. Fan, S. Freslon, C. Daiguebonne, L. L. Pollès, G. Calvez, K. Bernot, X. Yi, G. Huang, and O. Guillou, *Inorg. Chem.*, 2015, **54**, 5534–5546.
5. X. T. Rao, T. Song, J. K. Gao, Y. J. Cui, Y. Yang, C. D. Wu, B. L. Chen and G. D. Qian, *J. Am. Chem. Soc.*, 2013, **135**, 15559.
6. A. Cadiau, C. D. S. Brites, P. M. F. J. Costa, R. A. S. Ferreira, J. Rocha and L. D. Carlos, *ACS Nano*, 2013, **7**, 7213.
7. D. Zhao, X. Rao, J. Yu, Y. Cui, Y. Yang and G. Qian, *Inorg. Chem.*, 2015, **54**, 11193–11199.
8. Y. Q. Wei, R. J. Sa, Q. H. Li and K. C. Wu, *Dalton Trans.*, 2015, **44**, 3067.
9. K. Kumar, S. Chorazy, K. Nakabayashi, H. Sato, B. Sieklucka and S.-I. Ohkoshi, *J. Mater. Chem. C*, 2018, **6**, 8372-8384.
10. D. Wang, Q. Tan, J. Liu and Z. Liu, *Dalton Trans.*, 2016, **45**, 18450 —18454.
11. H.-Y. Wang, X.-Y. Zheng, L.-S. Long, X.-J. Kong, and L.-S. Zheng. *Inorg. Chem.*, 2021, **60**, 6790–6795.

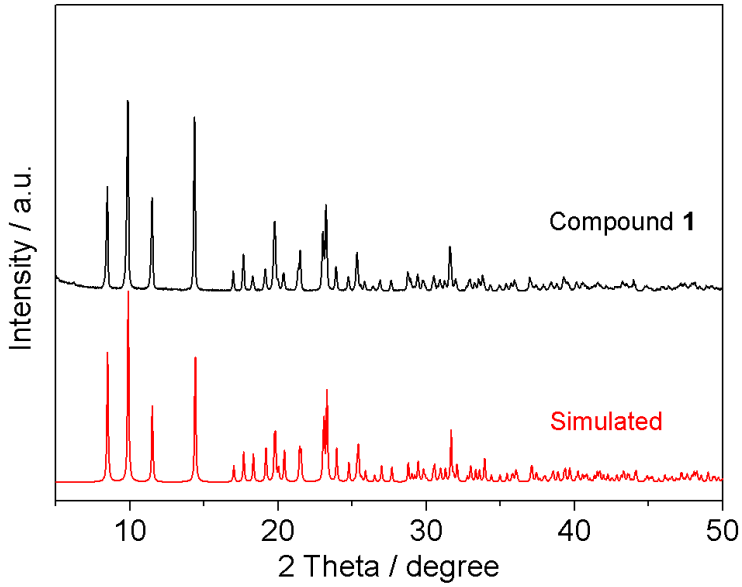

Fig. S1 Simulated and experimental PXRD patterns of **1**.

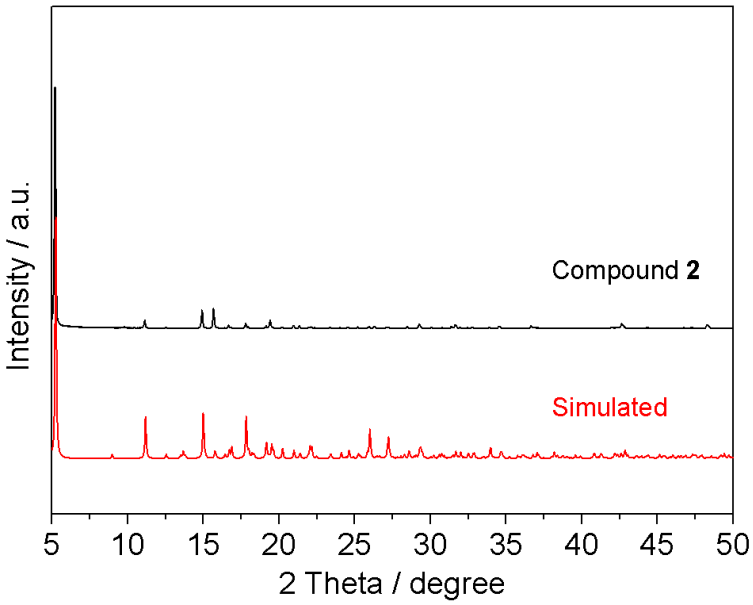

Fig. S2 Simulated and experimental PXRD patterns of **2**.

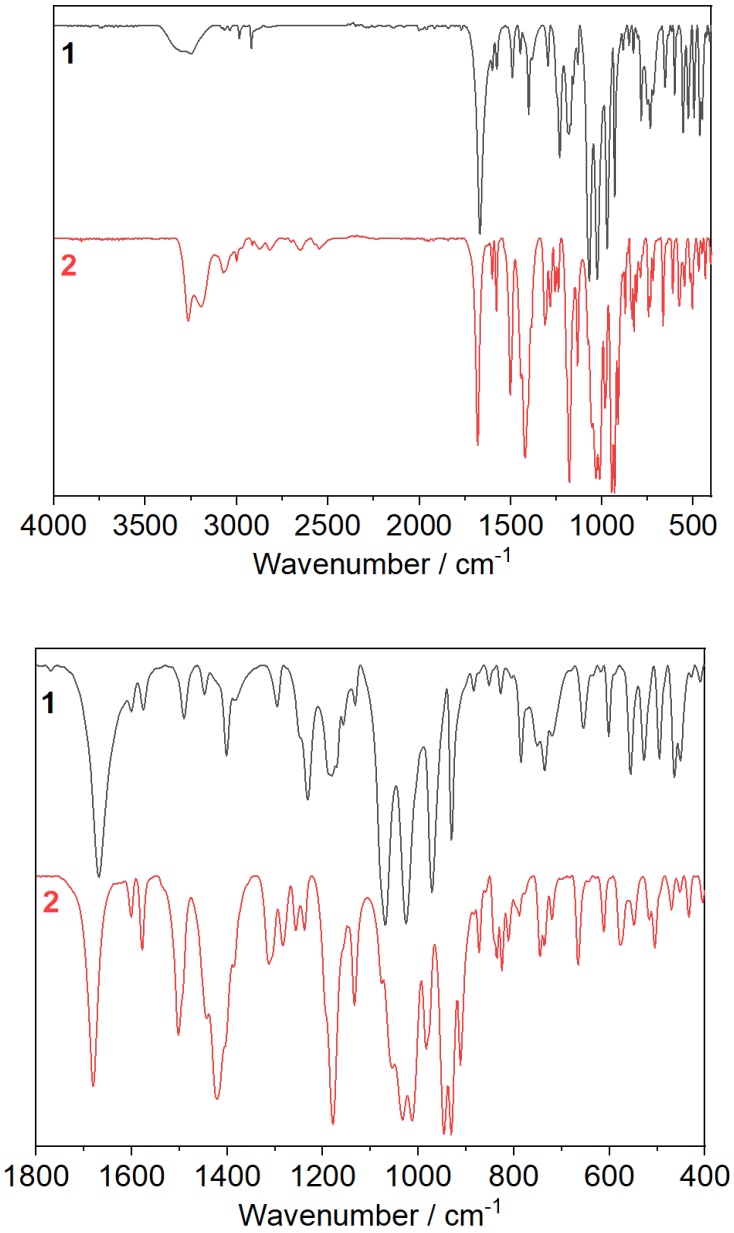

Fig. S3 The IR spectra of **1** and **2**. The peaks between 3390 cm^{-1} and 2962 cm^{-1} are assigned to the stretch of O-H from phosphonates and carboxylates. The peaks at 1000-1200 cm^{-1} are assigned to symmetric and asymmetric stretching vibrations of P-O and P=O. The peak at 930 cm^{-1} is assigned to the stretching vibration of U=O.

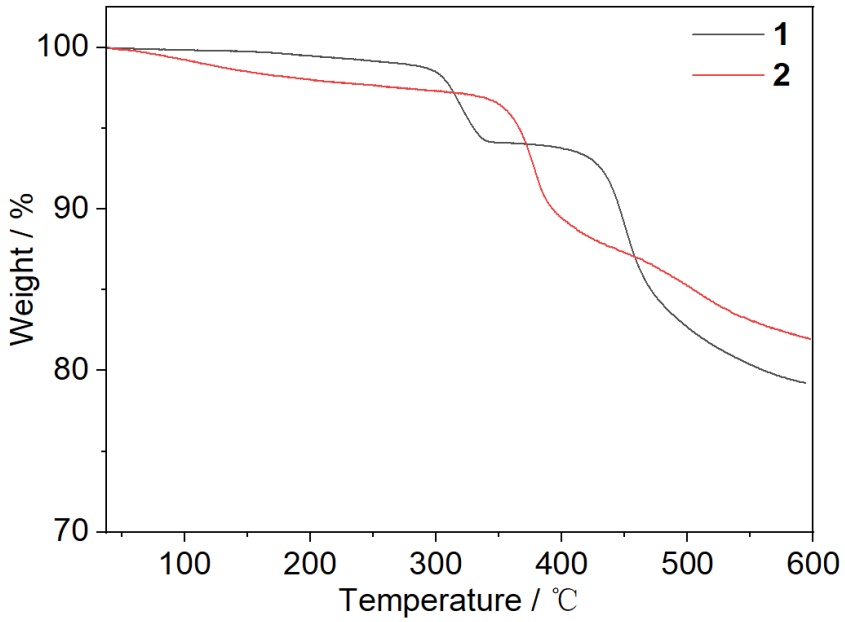

Fig. S4 Thermogravimetric analysis of **1** and **2**.

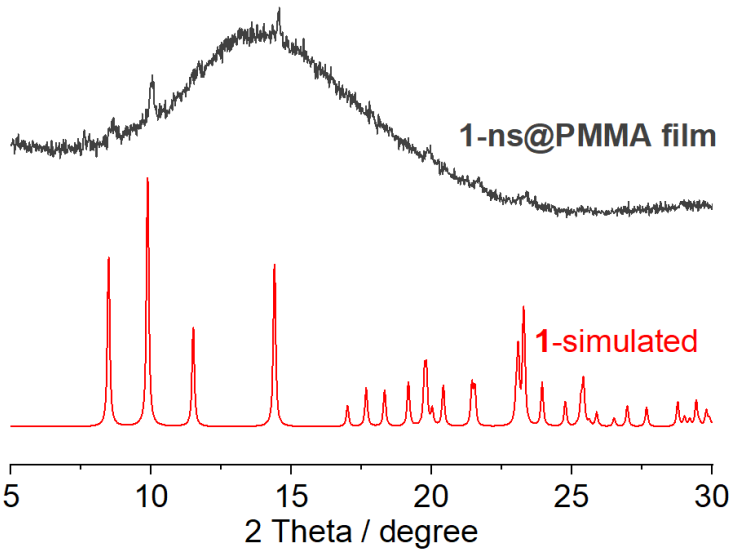

Fig. S5 The PXRD patterns of simulated **1** and **1-ns@PMMA film**.

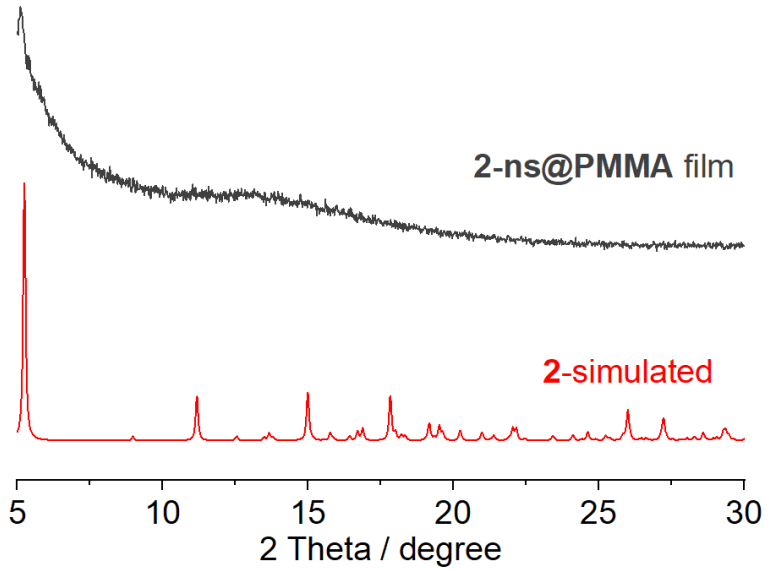

Fig. S6 The PXRD patterns of simulated **2** and **2-ns@PMMA film**.

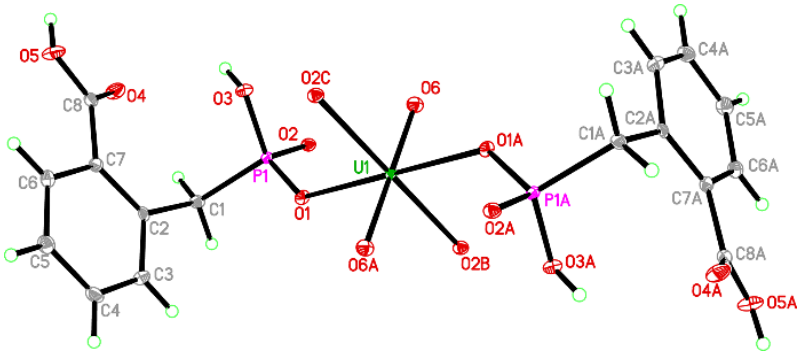

Fig. S7 View of compound **1**. Displacement ellipsoids are drawn at the 30% probability. level. A: -x+2, -y+1, -z; B: x+1, y, z; C: -x+1, -y+1, -z.

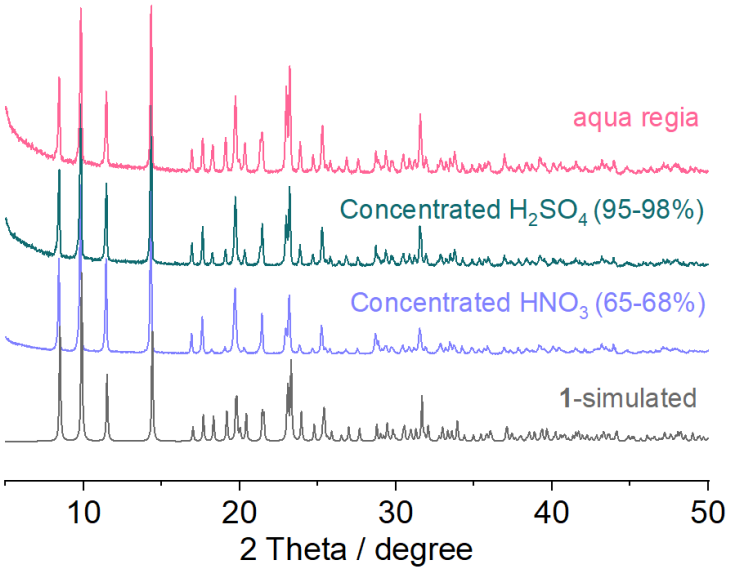

Fig. S8 The PXRD patterns for compound **1** after soaking in different acidic solution for 24 h.

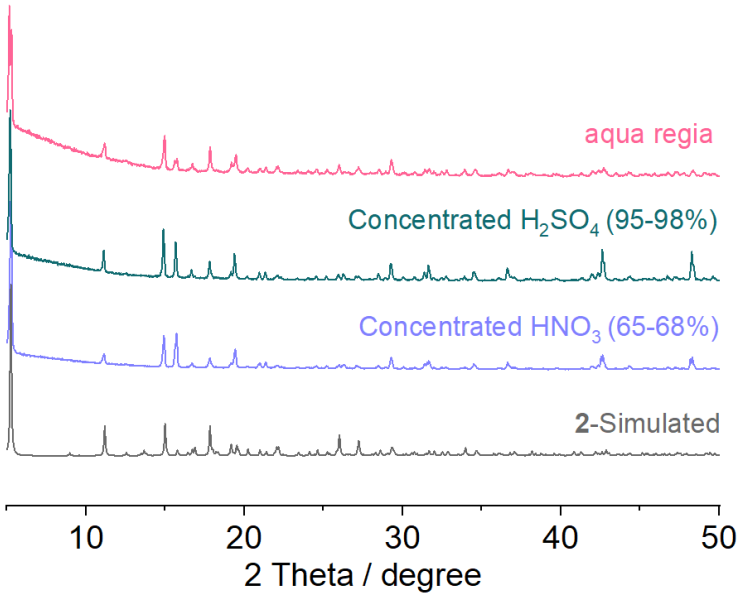

Fig. S9 The PXRD patterns for compound **2** after soaking in different acidic solution for 24 h.

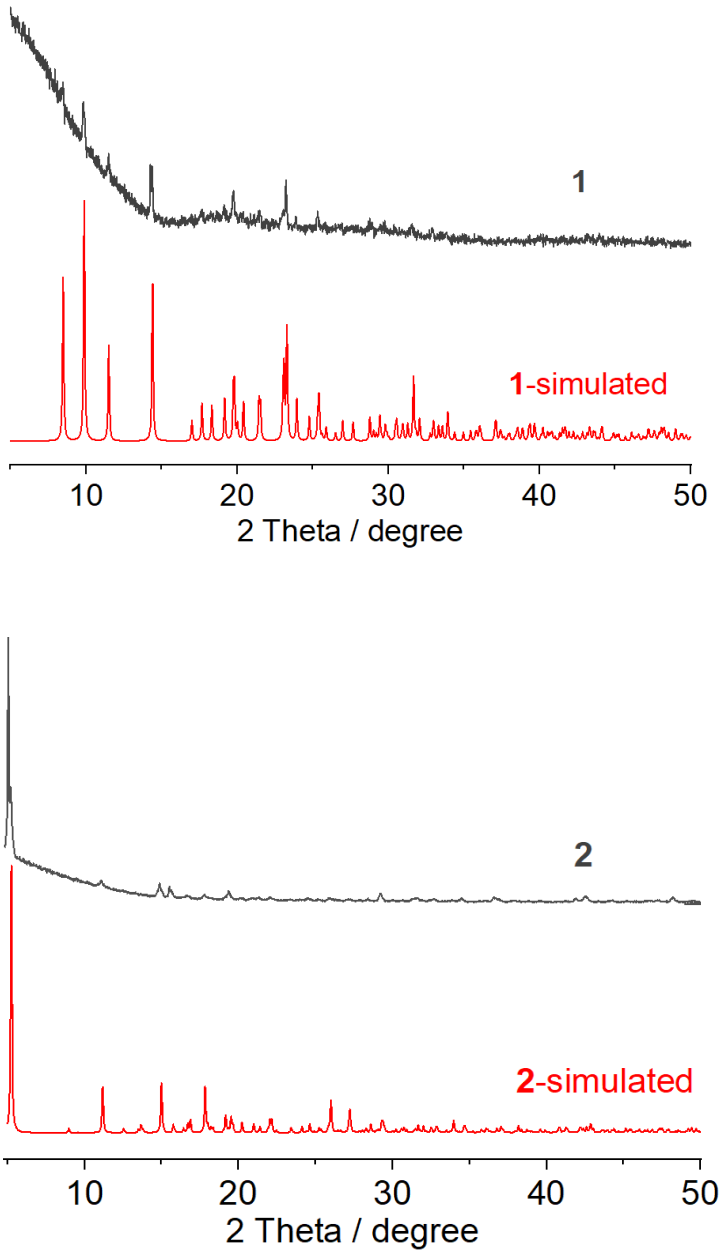

Fig. S10 The PXRD patterns of **1** and **2**, which represents the pristine sample dispersed in a pH = 11 solution, and the precipitate produced after adjusting pH = 2.

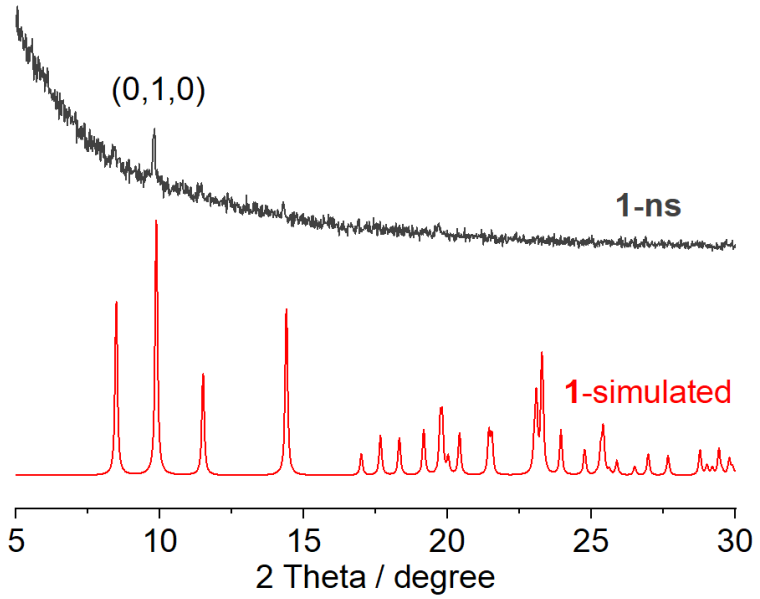

Fig. S11 The PXRD patterns of simulated **1** and **1-ns**, **1-ns** was obtained by volatilize the acetone solvent after freeze-thaw process.

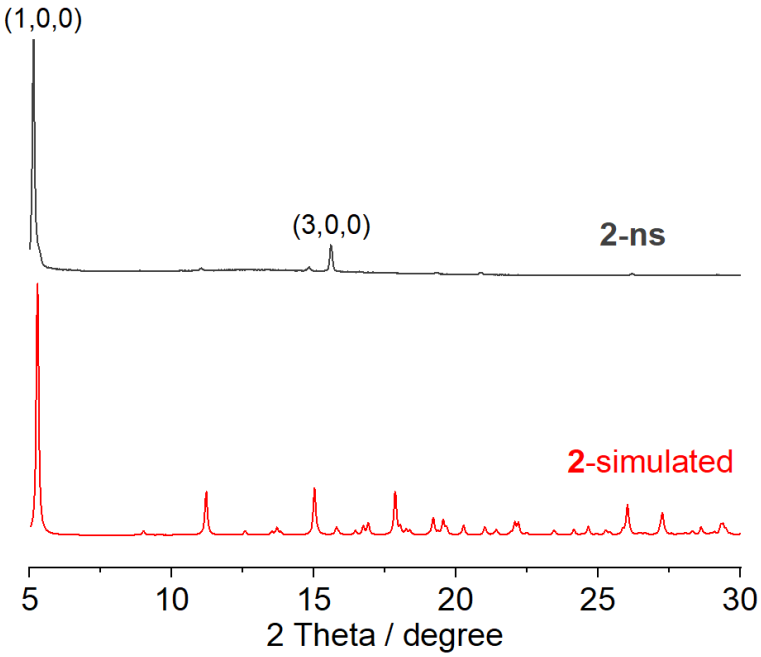

Fig. S12 The PXRD patterns of simulated **2** and **2-ns**, **2-ns** was obtained by volatilize the acetone solvent after freeze-thaw process.

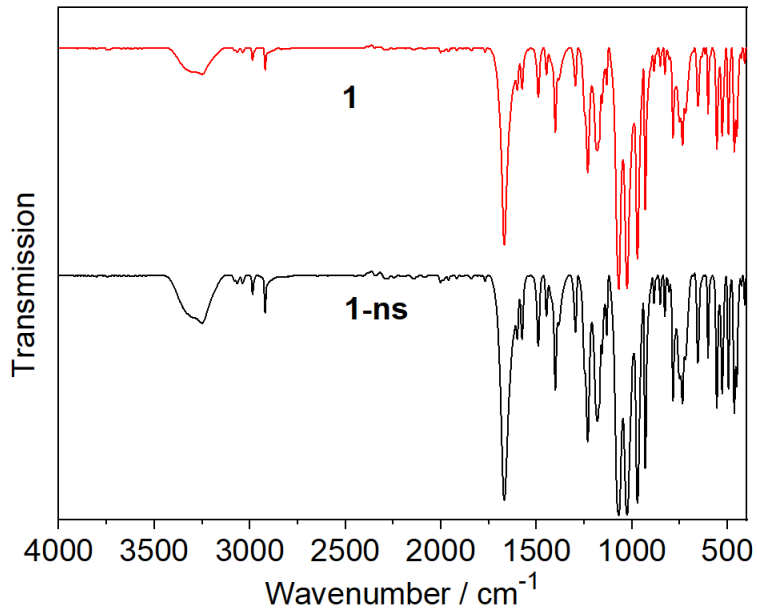

Fig. S13 The IR spectra of **1** and **1-ns, 1-ns** was obtained by volatilize the acetone solvent after freeze-thaw process.

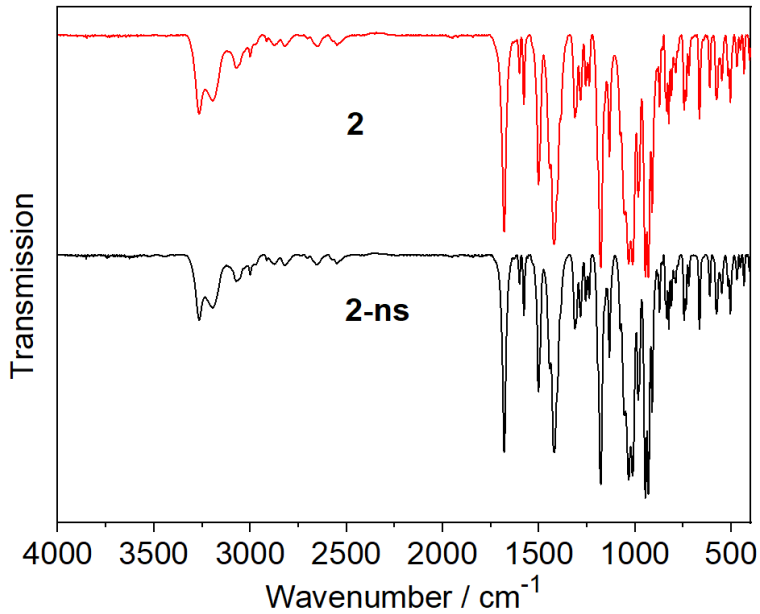

Fig. S14 The IR spectra of **2** and **2-ns**, **2-ns** was obtained by volatilize the acetone solvent after freeze-thaw process.

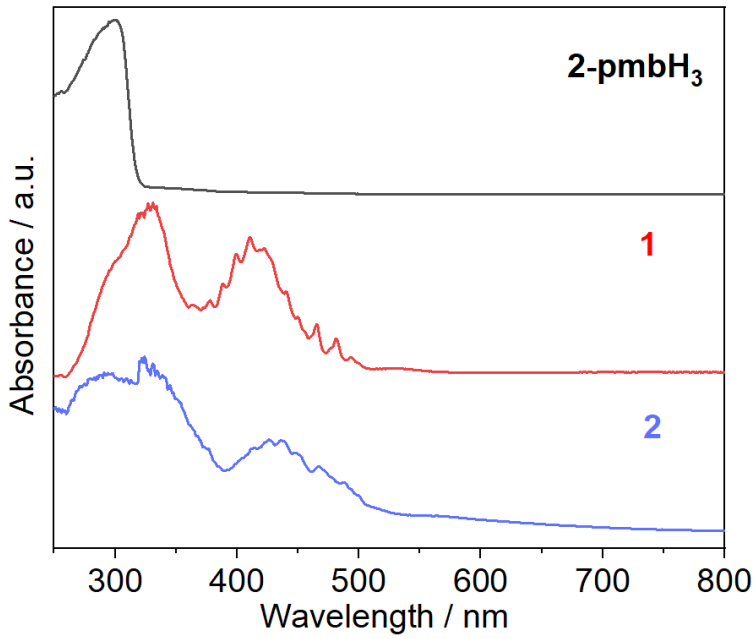

Fig. S15 Absorption spectra of 2-pmbH_3, **1** and **2**.

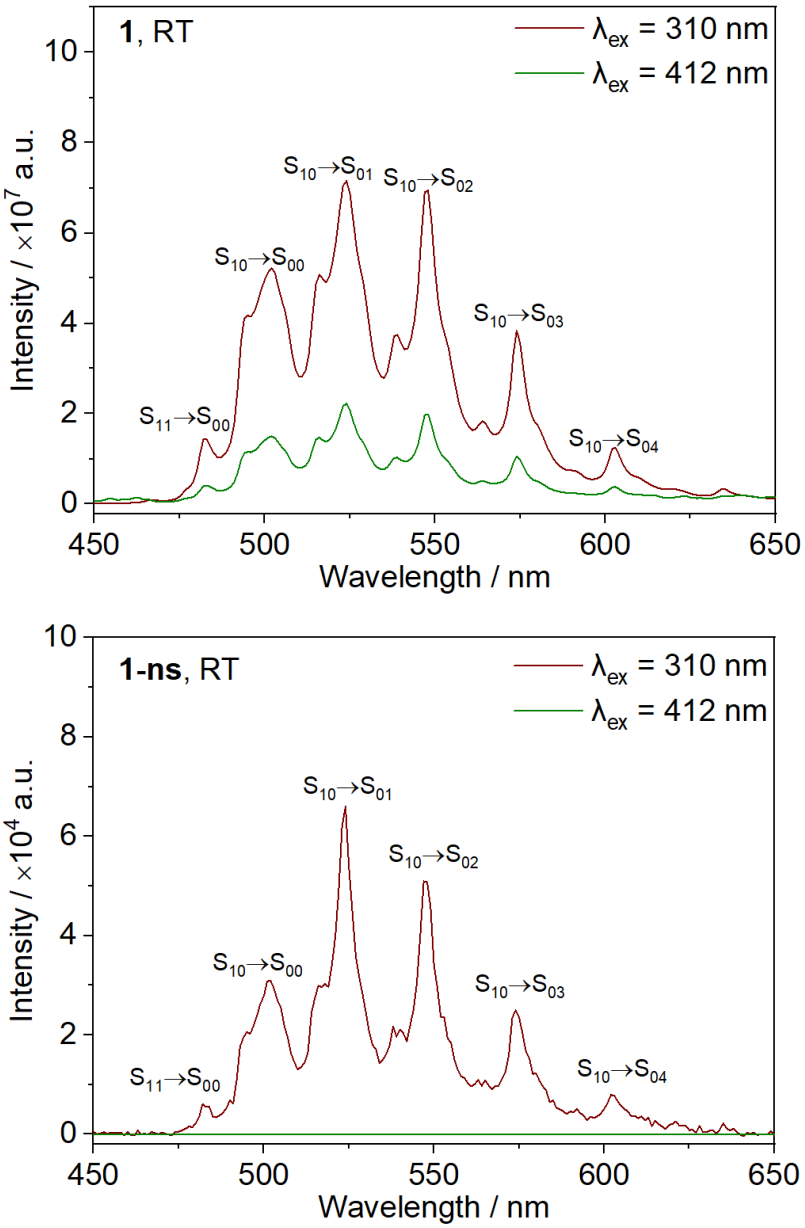

Fig. S16 Solid-state emission spectra of **1** and **1-ns** under excitation at 310 and 412 nm at room temperature.

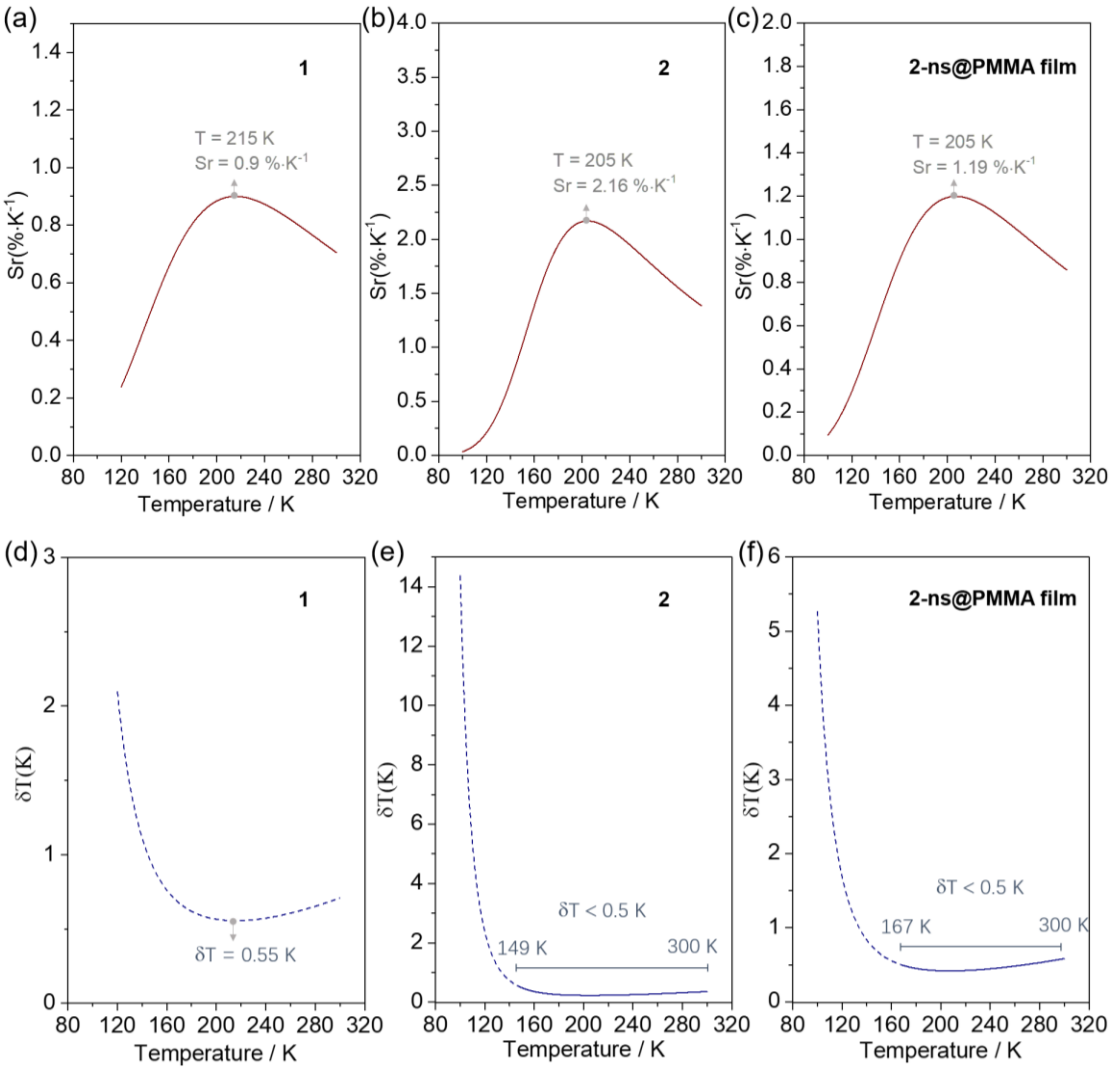

Fig. S17 a-c) Relative sensitivity of **1** in the 120–300 K range, **2** and **2-ns@PMMA** in the 100–300 K range. b-d) The minimum temperature uncertainty calculated from the sensitivity curve for $\delta\Delta/\Delta = 0.5\%$ ($\Delta = I_{(T)}/I_0$). The solid line represents the temperature uncertainty $\delta T < 0.5$ K.

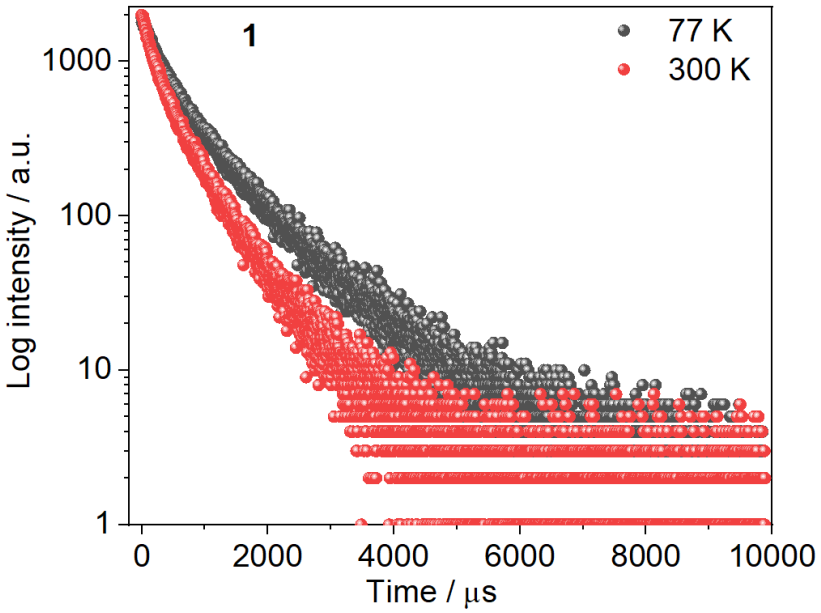

Fig. S18 Luminescence decay curves of **1** at 77K and 300K. (λ_{em} = 522 nm)

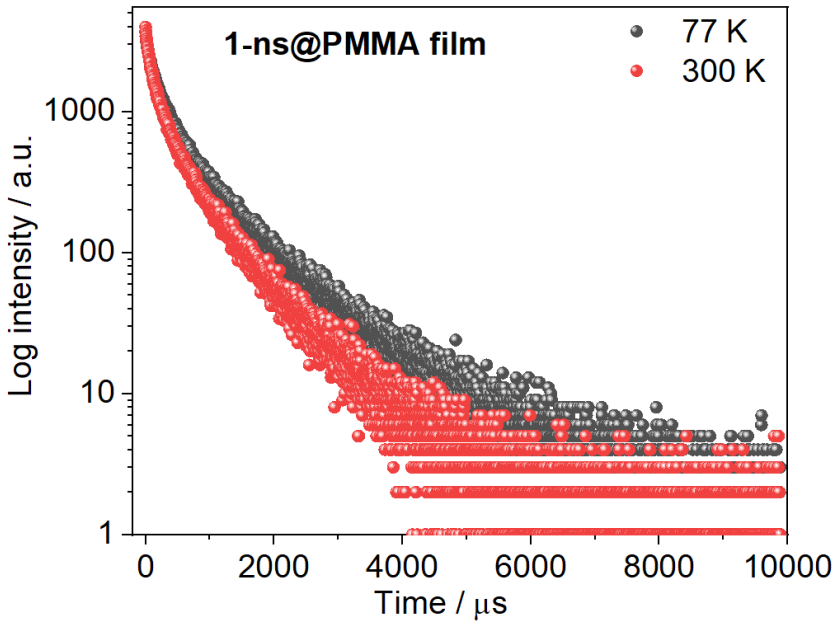

Fig. S19 Luminescence decay curves of **1-ns@PMMA** at 77K and 300K. (λ_{em} = 522 nm)

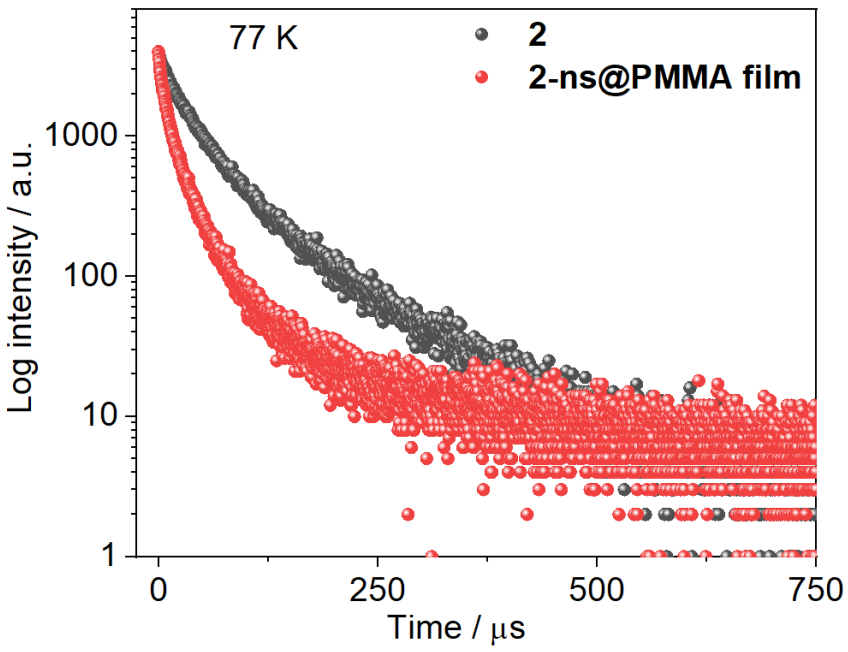

Fig. S20 Luminescence decay curves of **2** and **2-ns@PMMA** at 77K. (λ_{em} = 522 nm)

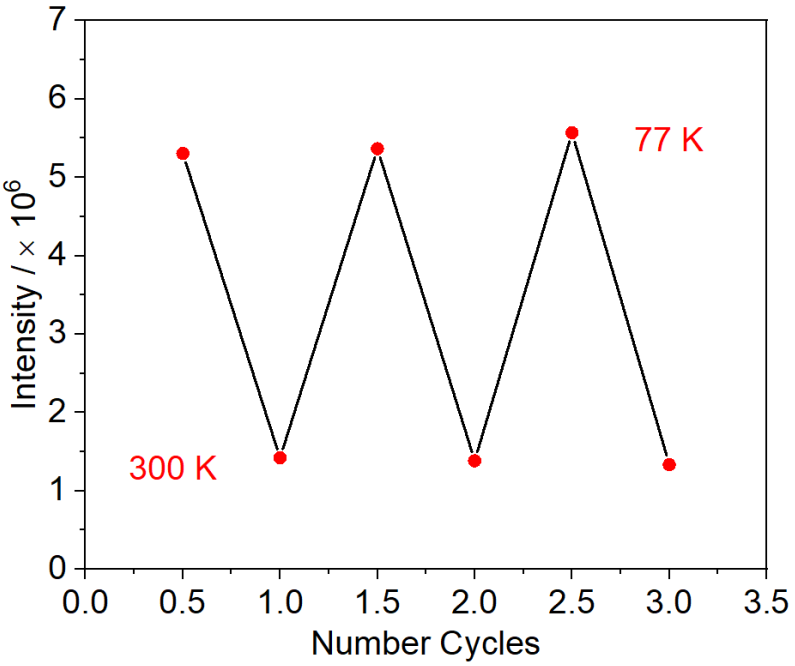

Fig. S21 Emission intensity of **1** at 522 nm in cycles of heating and cooling.